Bioresource Technology 394 (2024) 130173

Contents lists available at ScienceDirect

Bioresource Technology

journal homepage: www.elsevier.com/locate/biortech

Synergistic improvements in energy recovery and bio-oil quality through integrated thermochemical valorization of agro-industrial waste of varying moisture content

Madeline Karod [a], Samantha F. Rubin [a], Jillian L. Goldfarb [a,b,*]

[a] Department of Biological & Environmental Engineering, Cornell University 111 Wing Drive, Ithaca, NY 14853, USA
[b] Smith School of Chemical & Biomolecular Engineering, Cornell University, Ho Plaza, Ithaca, NY 14853, USA

HIGHLIGHTS

- Wet and dry wastes mixed in cascading thermochemical valorization pathways.
- Hydrothermal carbonization (HTC) as pyrolysis pretreatment enhances biochar HHV.
- HTC as pretreatment decreases biochar volatile matter beyond additive prediction.
- Mixing dry waste with hydrochar lowers acidity and O/C of pyrolysis bio-oil.

GRAPHICAL ABSTRACT

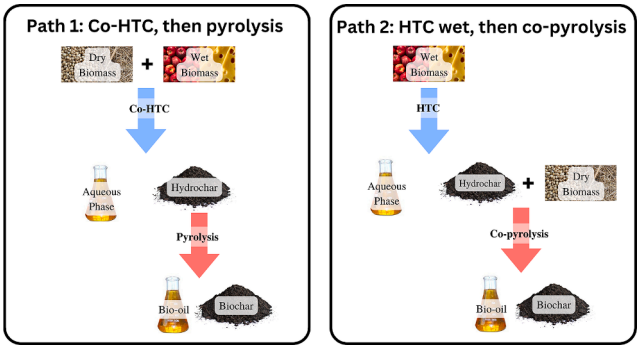

ARTICLE INFO

Keywords:
Hydrothermal carbonization
Pyrolysis
Synergy
Biochar
Biomass
Integrated biorefinery

ABSTRACT

Two thermochemical valorization schemes were investigated for co-upgrading dry and wet agricultural wastes through integrated hydrothermal carbonization (HTC) and pyrolysis. In the first pathway, dry and wet wastes were co-carbonized. The resulting hydrochar was pyrolyzed to yield an energy dense biochar (26–32 MJ/kg) high in fixed carbon (41–86 wt%) and low in volatile matter (6–12 wt%). The resulting bio-oil was lower in carboxylic acids and higher in phenols than predicted based on an additive scheme. In pathway two, wet waste (only) underwent HTC and the resulting hydrochar was mixed with dry waste and the mixture pyrolyzed. This pathway showed a lower biochar yield (32–67 wt%) and lower HHV values (24–31 MJ/kg) but higher fixed carbon content (65–84 wt%). The bio-oil contained more carboxylic acids than pathway 1 bio-oil. Pathway 1 biochars were more thermally reactive than pathway 2 biochars, reflecting a synergistic deoxygenation that occurs when incorporating dry waste in HTC prior to pyrolysis.

* Corresponding author at: Smith School of Chemical & Biomolecular Engineering, Cornell University, Ho Plaza, Ithaca, NY 14853, USA.
E-mail address: jlg459@cornell.edu (J.L. Goldfarb).

https://doi.org/10.1016/j.biortech.2023.130173
Received 8 September 2023; Received in revised form 25 November 2023; Accepted 6 December 2023
Available online 13 December 2023

1. Introduction

Composting and direct land-application of agricultural wastes are short-term carbon sequestration routes. Given biomass' instability, its land-application releases greenhouse gases upon decomposition (Liu et al., 2013a) and contributes to nutrient pollution through run-off (Dodds et al., 2009). Conversely, biorefineries can generate bio-products from agro-industrial residues (Farru et al., 2022; Goldfarb et al., 2017; Klemm et al., 2020). Thermochemical conversions, including pyrolysis and hydrothermal carbonization (HTC), convert organic matter into chars and bio-oils. Biochar (resulting from pyrolysis) and hydrochar (a product of HTC) can be upcycled into solid fuels, soil amendments, and water treatment materials, while pyrolysis bio-oil has a high energy density and can be upgraded to biofuel (Xiu and Shahbazi, 2012).

The choice of thermochemical treatment process and reaction conditions depends on the properties of the feedstock and the goal of treatment. For instance, HTC is well-suited to process high moisture wastes, as it leverages their water as the reaction medium. HTC concentrates carbon in the solid phase by reducing the feedstock's volatile matter, eliminating hydrogen and oxygen heteroatoms via hydrolysis, deoxygenation, and decarboxylation reactions, and imparting hydrophobicity to the hydrochar (Funke and Ziegler, 2010). Although HTC provides a clear valorization route for wet wastes, there are some notable drawbacks. Hydrolyzed compounds often recondense in the pores of the hydrochar during HTC, forming an amorphous "secondary char" phase (Kambo and Dutta, 2015). Hydrochar is comparable to low-value solid fuels like peat or a lignite coals in terms of its low heating value and low burn-out temperature (Silva et al., 2020). Finally, processing biomasses with low moisture contents via HTC is somewhat impractical as water would need to be added to the system.

Conversely, pyrolysis (devolatilization in an inert atmosphere) is well suited to upconvert dry biomasses to solid and liquid products. Biochar has a high fixed carbon content and is useful as an adsorbent for water treatment and soil amendment (Ahmad et al., 2014). Biochars can be substituted for coal in combustion scenarios due to their high fixed carbon content and porous nature, though biochars are not as energy dense and can have high ash content (Polin et al., 2019). Pyrolysis bio-oil is oxygenated, viscous and acidic, such that there is a pressing need for sustainable processing techniques to improve bio-oil quality (Xiu and Shahbazi, 2012).

Given the lack of a one-size-fits all process for agro-industrial wastes, and the drawbacks of each process individually, concurrent and integrated thermochemical treatment operations may facilitate the co-processing of multiple waste streams simultaneously. Co-treatment of different biomasses via HTC, pyrolysis, and other thermochemical methods can synergistically enhance the quality of final products (Anyaoha, 2022). For example, co-HTC of food waste and coal (1:1) synergistically increased the HHV and reduced the ash content of the resulting hydrochar (Ul Saqib et al., 2019). HTC can be used to pre-treat wet biomass prior to pyrolysis. A few studies have shown synergistic interactions by blending hydrochar with raw biomass as a feedstock for pyrolysis. Lin *et al.* showed that co-pyrolysis of cow manure hydrochar and agro-waste increased the surface area and nutrient availability of biochars and the concentration of phenols in bio-oil over what would be expected from a purely additive relationship of the feedstocks' resulting properties (Lin et al., 2021). Liu *et al.* found enhanced synergistic interactions between coconut shell hydrochar and lignite by increasing hydrochar ratios and pyrolysis temperatures (Liu et al., 2013b). Yao *et al.* found that blending paper sludge with green waste hydrochar promoted mass loss during pyrolysis (Yao et al., 2017). Pyrolyzing hydrochar may open its porous network by devolatilizing the secondary char present on the surface of the hydrochar to: (1) increase the surface area (Lin et al., 2021); (2) reduce thermal reactivity (Yao et al., 2017); (3) stabilize the final solid product (Zhou et al., 2023); (4) de-oxygenate the bio-oil.

However, the studies mentioned do not ask an important question: when and how should wet and dry biomasses be mixed to exploit synergistic interactions? This work couples HTC and pyrolysis to generate liquid and solid fuel products from heterogeneous waste streams. Two thermochemical treatment pathways were studied that differ in whether both (wet + dry) wastes were incorporated during HTC and through to pyrolysis, or if the wet waste is first processed via HTC and then the hydrochar combined with a dry waste during pyrolysis. In the first pathway two biomass wastes were combined and co-treated via HTC, and the resulting hydrochar was pyrolyzed. In this pathway, the wet/dry biomass ratios were 90/10 and 80/20 (by mass) so as to leverage the moisture content in the wet biomass and reduce the need to add fresh water. In the second pathway one wet biomass waste was treated using HTC, and the resulting hydrochar was combined with a second (dry) waste and co-pyrolyzed. In this pathway, the HC/dry biomass ratios were 20/80 and 50/50, which allows for use of a range of HC compositions and dry wastes without being limited by water content. The resulting biochars were then assessed for their potential solid fuel applications.

2. Materials and methods

Four biomass wastes representative of the Finger Lakes region in New York (NY) were selected; these wastes were previously studied as independent HTC or pyrolysis feedstocks (Dimitriadis et al., 2023; Pecchi et al., 2022; Pollard and Goldfarb, 2021; Zhang et al., 2018). The wastes include apple pomace (AP) from apple cider/juice production, sweet dairy whey (DW) from cheese production, cherry pits (CP) from cherry processing, and barley straw (BS) from beer production. The moisture content of the feedstocks was an important factor in their selection. Two feedstocks, DW and AP, have a high moisture content (>75 %) suitable for HTC, and BS and CP have a low moisture content (<10 %), which likely renders them more suitable for pyrolysis or in a blend with wet feedstocks for HTC. Moisture contents were determined by drying biomass at 105℃ and weighing to constant mass.

Ruby Frost apples (Malus domestica) grown in NYS were skinned, cored, pulverized, and pressed to generate AP. DW was obtained from the Cornell Dairy in Ithaca, NY. AP and DW were stored at −4℃ and defrosted prior to experimentation; no pretreatment was performed on the wet biomass. CP from United States tart cherries (*Prunus* cerasus) were acquired from the Great Lakes Packing Company in Kewadin, MI where they were dried at 120 °C for 1 h then stored in a grain silo. Upon receipt, CP were rinsed in DI water and dried at ambient laboratory conditions (room air temperature of 22 °C) then ground and sieved to a particle size of 250–500 μm. BS was recovered from the Musgrave Research Farm in Aurora, NY and stored at ambient conditions. BS was processed to shorten the straw pieces to 1–2 cm in length in a blender.

2.1. Hydrothermal carbonization of feedstocks

For each HTC run, a 1-L Parr Series 4525 Bench Reactor equipped with a 4848 Parr Controller (schematic available in Supplemental Information) was loaded with either one of the wet wastes (100 % DW or 100 % AP) or one of four combinations of one wet and one dry waste [(DW or AP) + (BS or CP)]. Dry and wet wastes were hand-mixed using a spatula in the reactor and water was then added and the mixture was stirred again. For the AP-containing mixtures, deionized water was added to reach a biomass:water ratio of 0.15. For the DW mixtures, the biomass:water ratio was greater than 0.15 without the addition of water due to the high moisture content of DW (97 wt%), while AP mixtures had a biomass:water ratio of 0.15 as AP has a moisture content of 80 wt %. Though biomasses were all mixed in the same proportions (80/20 or 90/10 wet/dry), these ratios result in different dry basis biomass: biomass ratios due to the differing moisture contents of the feedstocks (determined via drying in an oven at 110 °C to constant mass). The reactor was filled to approximately 50 % capacity (by volume) with the

500 g of water and feedstock used for each run.

The reactor was flushed with high purity nitrogen three times, and then pressurized to 0.55–0.57 MPa as was done in previously published work using this reactor as it was found to keep all biomass submerged in water and eliminate oxygen from the system (Pecchi et al., 2022). The reactor was heated at an average rate of 2.6℃/min (±0.8℃/min). Upon reaching 220℃ ± 3 °C, the temperature was maintained for one hour. This temperature was chosen as it is in the middle of the carbonization temperature range (180-250℃) and would ensure carbonization would proceed without entering the liquification regime (250-370℃) (Cao et al., 2021). Throughout the experiment, the reactor was stirred at 400 RPM (chosen based on methodology from Pecchi et al., 2022). Following carbonization, the reactor was quenched in an ice bath until it reached 20℃. The average cooling rate was 10.5℃/min, with a standard deviation of 3.8℃/min. Hydrochar was separated from process water via vacuum filtration on cellulose filter paper (Whatman, 45 μm). Hydrochar was dried at 110℃ in a laboratory oven to constant weight, and then stored at room temperature. To determine the yields of hydrochar, process water, and gas, the mass of the process water extracted during vacuum filtration was recorded, and the mass of the dried hydrochar was subtracted from the mass of the wet hydrochar to determine the total process water. The mass of the dried hydrochar and the total process water was divided by the total mass added (~500 g). The gas yield was calculated using the pressure difference from before heating and after quenching and applying the ideal gas law to the reactor head space above the condensed phases. Loss was calculated by difference.

2.2. Pyrolysis

In pathway 1, both pure and mixed hydrochars were pyrolyzed. In pathway 2, DW or AP hydrochars were mixed with raw dry biomass. We proposed the ratios chosen for pathways 1 and 2 to reflect industrially relevant scenarios. In pathway 1, if a large proportion of dry waste was carbonized, significant additional water would be required to achieve a suitable B:W content for HTC. In pathway 2, the mixing ratios chosen were 20/80 and 50/50 wet waste hydrochar/dry biomass. These ratios complement the dry biomass/biomass ratios in pathway 1 since the hydrochars and the dry biomass feedstocks have comparable moisture contents. Given the large volume reduction of wet waste during HTC, larger quantities of dry waste are likely more readily available than hydrochar, so mixtures with large proportions of hydrochars may be less viable. Given the time-consuming nature of this work, a selection of samples from different pathways, feedstocks, and mixing ratios were duplicated with averages and ranges reported. We note that these combinations of biomasses are intended to demonstrate a proof-of-concept and explore possible synergistic behaviors during co-treatment in coupled thermochemical processes. Future work should explore (1) optimal mixture ratios as a function of feedstock availability, product quality, etc. and (2) align feedstock and process selection to enhance the technoeconomic feasibility of such integrated biorefineries (Kassem et al., 2022).

Samples were pyrolyzed in a porcelain boat in an MTI GSL-1100X 2″ horizontal fixed bed tube furnace under nitrogen flowing at 100 mL/min (Parker Balston generator, >98 % purity). Samples were dried at 110 °C for 30 min, then heated to 600 °C at 10 °C/min and held for 60 min. The condensable bio-oil was collected using two cold traps submerged in a dry ice and glycol mixture (between 7 and 11 °C). The cold traps were measured before and after bio-oil collection to determine the mass of bio-oil collected. The boat was removed once the furnace cooled to below 100 °C and the weight of the empty boat was subtracted from the weight of the boat + biochar to determine mass of biochar. The mass of the bio-oil and biochar were divided by the initial mass of the biomass to determine liquid and solid yields, respectively. The gas yield was determined by difference.

2.3. Analysis of bio-oil

The cold traps were weighed directly after pyrolysis to determine the amount of oil produced. 10 mL of dichloromethane (DCM) was then added to cold traps to extract the oil. The extracted oil was analyzed on a Shimadzu GC 2010 Plus gas chromatograph-mass spectrometer (GC–MS) with AOC-20i autosampler on a crossbond 30 m long 0.25 mm ID silica column. Samples were injected with a 15:1 split ratio at 250 °C at an initial oven temperature of 40 °C, purged with 1 mL/min of helium (Airgas UHP-300). The oven was held at 40 °C for 5 min, then ramped at 5 °C/min to 150 °C where it held for 5 min. The oven temperature was increased at 1.75 °C/min to 250 °C with a final 10-minute hold. The mass spectrometer scanned between 15 and 400 m/z after a 6-minute solvent cut time. The resulting peaks were filtered (slopes $\geq$ 900, duration $\geq$ 2 s) and identified by matching spectra with the internal NIST libraries. The GC–MS was calibrated with 26 marker compounds that are common to the thermochemical conversion of lignocellulosic biomass (detailed in SI). The atomic ratios of the bio-oil were calculated stoichiometrically from the concentrations of compounds identified by the GC–MS.

2.4. Char characterization

Proximate analysis and oxidative differential thermogravimetric analysis (DTG) were conducted using a TA Instruments Thermogravimetric Analyzer (TGA) SDT 650 Discovery. For proximate analysis, samples were heated under nitrogen at 10 °C/minute to 110 °C and held for 30 min to determine the moisture content. Then, samples were heated at 10 ℃/min to 900 ℃ and held isothermally for 30 min to determine the volatile matter. Then, the gas was switched to air, heated to 950℃ at 10℃/min and held for 30 min to oxidize the organic matter (fixed carbon). The remaining inorganic matter is referred to as ash. Each sample was run at least twice, and up to four times (for biochar samples produced in duplicate).

For oxidative DTG analysis, samples were heated under nitrogen at 10℃/minute to 110 ℃, and held isothermally for 30 min to eliminate moisture. Next, the gas was switched to air, heated at 10 ℃/min to 950 ℃ and held for 30 min. Peak reactivity was determined via DTG curves by differentiating fractional mass at any time, t, with respect to temperature at that time, starting with a dry baseline.

A CE-440 Elemental Analyzer (Exeter Analytical Inc.) was used to determine the elemental analysis (C, H, N, and O by difference) of samples, which were run in triplicate. The higher heating value (HHV) of the sample was calculated based on the ultimate analysis (available in Supplemental Information) according to the modified Dulong's Equation (Shi et al., 2016), one of the most widely-used equations for estimating the heating value of carbon materials (Chen et al., 2022; Jiang et al., 2022; Mondal et al., 2023):

$$HHV\left(\frac{MJ}{kg}\right) = 0.353\mathrm{C} + 1.01\mathrm{H} - 0.13\mathrm{N} - 0.0818\mathrm{O} \quad (1)$$

2.5. Analysis of synergistic behavior

The hypothesis tested here is that co-processing of wet and dry biomass (by combining them during HTC or via cascaded processing of producing hydrochars from wet biomass and combining them with dry biomass followed by pyrolysis) will lead to synergistic reaction behavior. The opposite of synergistic behavior is "additive" behavior. We calculate the additive values for each mixture based on a weighted fraction of the single-biomass sample results. Equation (2) shows how additive values of a given char characteristics, A, (e.g. HHV) are predicted based on an additivite combination of the values obtained from pure biomass samples that underwent the same process.

$$A = A_1{}^*X_2 + A_1{}^*X_2 \quad (2)$$

In Equation (2), A_1 and A_2 are the experimental values of the wet and dry biomasses' characteristics, respectively, and X_1 and X_2 are the respective proportions of wet and dry biomass included in each mixture. When calculating an additive ratio (e.g. O/C and H/C ratios), the additive values for the numerator and denominator were calculated and subsequently divided.

For pathway 1, the pure biomass feedstocks (A_1, A_2) used were biochars resulting from the individual wet and dry biomass that was hydrothermally carbonized and then pyrolyzed (referred to as AP HC, DW HC, CP HC, and BS HC). For pathway 2, $A_1$and A_2 represent the pure feedstock biochars from wet biomasses that were hydrothermally carbonized and then pyrolyzed, and biochar from dry waste that was only pyrolyzed (AP HC, DW HC, CP, and BS).

3. Results and discussion

This work considers two valorization pathways of two wet and two dry wastes to determine the relative solid and liquid fuel values produced when (1) both wet and dry wastes are pretreated with HTC and subjected to pyrolysis or (2) wet wastes are converted to hydrochar and mixed with raw dry waste prior to pyrolysis.

3.1. Yields of pure and mixed feedstocks from HTC, Pyrolysis, and pathways 1 and 2

The four pure feedstocks and the Pathway 1 mixtures were each subjected to hydrothermal carbonization at 220 °C for one hour. Hydrochar yields for the various mixtures ranged from 16 wt% to 51 wt % as reported in Fig. 1a. Losses were < 2 % on average; data are reported on a loss-free basis. For the mixtures, the HTC process water decreases compared to pure feedstocks (Fig. 1a). Pure DW HC saw a small increase in solid (hydrochar) yield from approximately 3 wt% raw solid content to 6 wt% after HTC, which suggests secondary char formation, *i.e.*, a recondensation of organic compounds on the surface of the hydrochar that were dissolved in the aqueous medium.

The yields from the pyrolysis of raw dry wastes, single feedstock hydrochars, and mixtures from pathways 1 and 2 are reported in Fig. 1 (full data in Supplemental Information). Overall, pathway 1 biochars showed higher yields than pathway 2. This was expected, as in pathway 1 dry waste was pre-treated via carbonization and pyrolyzed as a hydrochar. Hydrochars have significantly higher fixed carbon than their parent biomasses due to the decarboxylation and dehydration reactions that dominate the HTC process, removing volatile matter (Bardhan et al., 2021). This effect can also be seen in the pure biochars: dry wastes subjected to HTC followed by pyrolysis (CP HC and BS HC) had higher

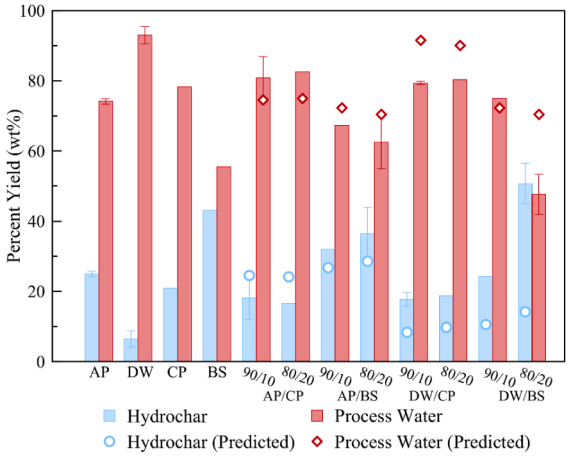

a. Product yields and predicted values resulting from hydrothermal carbonization for pure feedstocks and pathway 1 mixtures

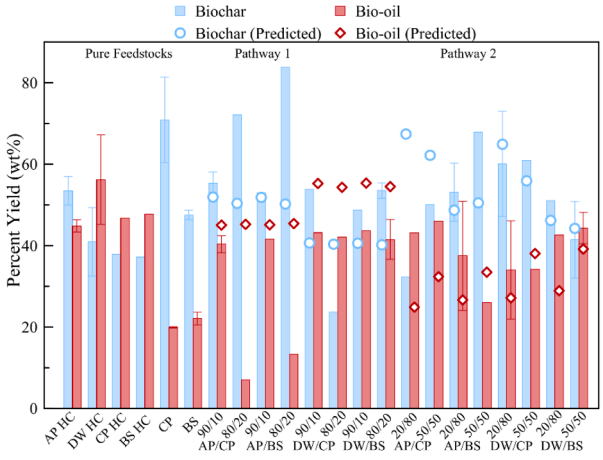

b. Pyrolysis yields of pure feedstocks and pyrolysis yields and predicted values from pyrolysis step of pathway 1 and pathway 2 mixtures

Fig. 1. Product yields and predicted values across pathway 1 and 2. (Average of two runs with standard deviation reported when replicates available).

solid yields than dry wastes only subjected to pyrolysis (CP and BS).

Due to the increased fixed carbon content in the hydrochars, it was expected that increasing the proportion of dry waste would decrease the solid yield, which was confirmed. For instance, the solid yield of an AP/CP 90/10 mixture (pathway 1) was 40.4 %, but when increasing the dry waste to AP/CP 80/20, the solid yield was 34.2 %. In pathway 2, the mixtures were either 80 % raw dry waste / 20 % wet-waste hydrochar, or 50/50. Because the dry wastes were not pre-treated, they contained (relatively) less fixed carbon and more volatile matter than their carbonized counterparts. Pathway 2 may therefore be more useful to enhance bio-oil recovery as bio-oil originates from the volatile matter.

Pyrolysis solid yields also depend on the biomass. Biochars from pathway 1 made with AP show lower biochar yields than predicted using the additive scheme of Equation (2), particularly when increasing the dry waste content. This suggests that HTC is less effective at carbonizing mixtures of AP and dry waste than the individual biomasses, such that more devolatilization occurs during pyrolysis, leading to a lower solid biochar yield. Samples including DW have a significantly higher ash content than samples with AP. This is expected, as 8–10 % of the solids in whey are inorganics, mostly calcium and magnesium (Renhe et al., 2019). Since DW has a moisture content of 97 %, the hydrochar yield is low, such that pathway 2 might not be feasible for DW treatment. However, co-HTC of DW with another waste, as in pathway 1, increases the hydrochar yield and leverages the DW moisture content as the reaction medium.

3.2. Biochar characterization

All biochars showed comparable fixed carbon (>50 wt%, except 80 DW 20 CP at 41 wt%) and volatile matter contents (<13 wt%) to high rank coals (Fig. 1) ("Proximate Analysis," 2015). Biochars had significantly higher fixed carbon and lower volatile matter contents than hydrochars, which is a result of the devolatilization of the solid during pyrolysis. Biochars in pathway 1 have more ash than biochars in pathway 2. Ash content can be reduced as some inorganics enter the aqueous phase during HTC (Reza et al., 2013). By contrast, in pyrolysis, inert matter primarily remains in the solid phase, causing the ash content to be higher in the biochar than raw feedstocks. Hydrochar has significantly less volatile matter as compared with raw biomass, so incorporating dry waste in HTC, as in pathway 1, decreased volatile matter and increased the fixed carbon in the final char, though ash was generally higher than pathway 2.

Previous studies show a link between lignin content, fixed carbon content, and energetic density. In general, mixtures incorporating CP have a higher HHV than mixtures incorporating BS. This is attributed to the higher lignin content of CP (33 % lignin (Cruz-lopes et al., 2022)) compared to BS (approximately 14 % lignin (Sun et al., 2011)), as lignin has a higher calorific value than cellulose or hemicellulose (Kambo and Dutta, 2015). AP and DW are cellulose-based and have negligible lignin content, thus the HHV and fixed carbon content being dictated by the CP and BS content in the mixtures.

The HHV for pathway 1 range from 26 to 32 MJ/kg, with AP mixtures showing higher values than DW mixtures (Fig. 2). Values for pathway 2 range from 24 to 30 MJ/kg, with the DW/BS mixtures producing the lowest HHV values. The higher HHV for pathway 1 is likely a result of the two stages of carbonization for both wastes, which enhances deoxygenation and increases fixed carbon content (Fig. 2). This is also shown in the HHV of pure biochars. The HHV of dry waste that has been treated with HTC and pyrolysis (CP HC and BS HC) is greater than the HHV of dry waste that has only been treated with pyrolysis (CP and BS).

The O/C and H/C atomic ratios of the biochars were investigated to determine if either pathway was effective in deoxygenating the biochar to its solid fuel potential. The O/C ratios range from 0.08 to 0.22 for pathway 1, with AP/CP mixtures having the lowest O/C atomic ratios and DW/BS having the highest. This is also true for pathway 2, where values range from 0.11 to 0.28. The H/C values range from 0.19 to 0.22 and 0.19–0.24 for pathways 1 and 2, respectively. In the context of solid fuels, these values are both low, which, for the O/C ratios is advantageous, and there is a notable decrease in both O/C and H/C atomic ratios for biochar mixtures from the pure biochars (Fig. 2). This is indicative of dehydration and deoxygenation reactions occurring during pyrolysis, likely coupled with demethylation reactions, and the degree is unchanged between pathway 1 and 2.

Oxidative DTG analysis sheds insight into the potential to use biochars as a combustible solid fuel. Oxidative DTG curves of biochars are shown in Fig. 3. Curves for all biochars are similar in shape, showing one major peak in reactivity, ranging from 402 °C to 620 °C. For biochars in pathway 1, peaks typically occur at higher temperatures than pathway 2. This indicates that incorporating dry waste in HTC pretreatment leads to a reduced oxidative reactivity of the resulting biochar. Biochars with BS showed a consistently lower temperature of peak reactivity than CP. Overall, biochar samples from both pathways containing BS had a lower temperature for peak reactivity which indicates that these materials would be the most energetically efficient amongst the samples produced. The data also suggests that the mixing ratio has a relatively small impact on the biochar solid fuel potential.

3.3. Pyrolysis bio-oil composition across pathways

To organize the product distribution of bio-oil produced across the two pathways and feedstock mixtures, bio-oil compounds were classified into 8 functional groups: alcohol, aldehydes, benzenes, carboxylic

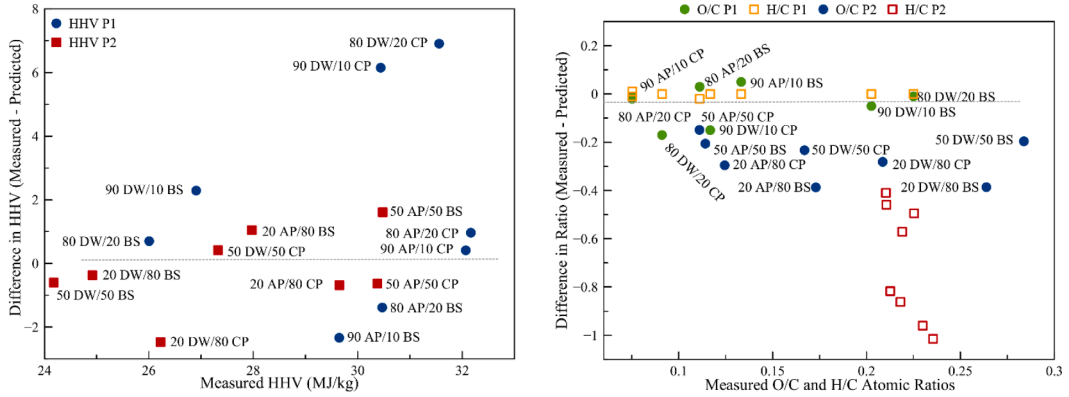

a. HHV of mixtures

b. Residual plot of O/C and H/C atomic ratios (O/C ratios labelled for both pathways)

Fig. 2. Evidence of deoxygenation of biochars through HHV and O/C and H/C ratios, synergistically enhanced via pathway 2.

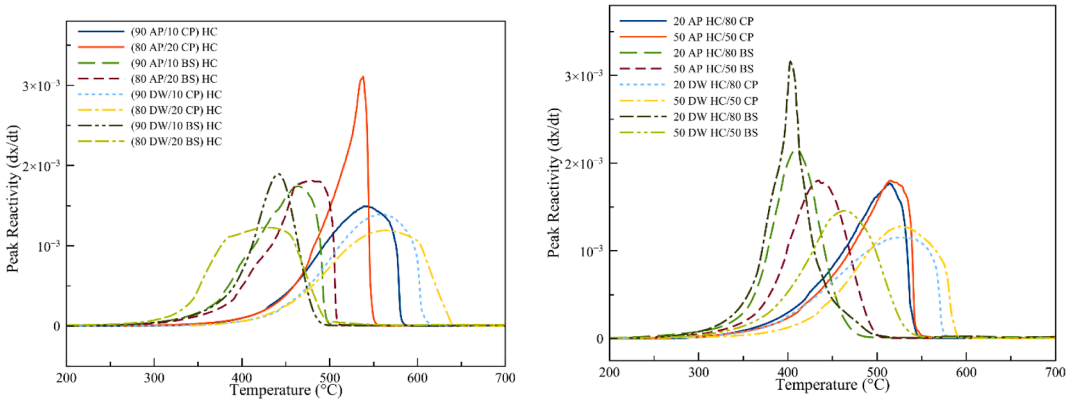

a. Oxidative DTG curves for biochars made via pathway 1

b. Oxidative DTG curves for biochars made via pathway 2

Fig. 3. Oxidative derivative thermogravimetric curves of biochars highlighting higher peak reactivity for CP-based mixtures from both pathways and reduction in peak reactivity for pathway 2 versus pathway 1.

acids, esters, furans, hydrocarbons, ketones, pyrroles, and phenols (Fig. 4). Aldehydes, esters, hydrocarbons and pyrroles were omitted from the figure due to low concentration (<5 ppm; all bio-oil data available in Supplemental Information). We note that experimental constraints enabled only one GC–MS analysis of the bio-oil per sample. As such, we analyzed the bio-oil in terms of overall functional group

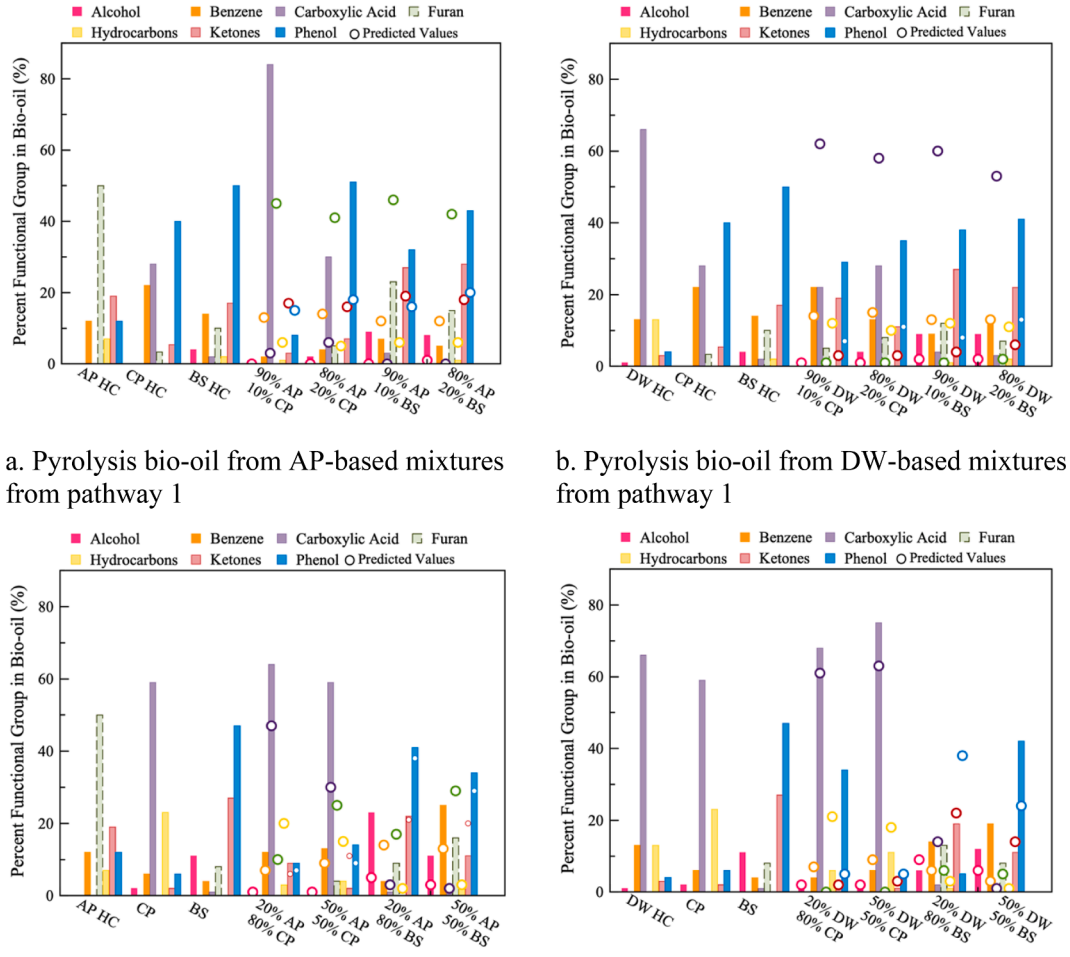

a. Pyrolysis bio-oil from AP-based mixtures from pathway 1

b. Pyrolysis bio-oil from DW-based mixtures from pathway 1

c. Pyrolysis bio-oil from AP-based mixtures from pathway 2

d. Pyrolysis bio-oil from DW-based mixtures from pathway 2

Fig. 4. Composition of bio-oil produced from AP- and DW-based mixtures from pathway 1 and pathway 2 broken into functional groups and compared to predicted values.

compositions and did not focus on yields of specific components, nor do we claim statistically significant differences exist between many values. However, the data reveal more substantial differences among some mixtures/pathways than others. This, combined with knowledge of the feedstock composition, volatile matter content and reaction pathways in the literature provide a unique picture of where future research could go to capitalize on reaction synergies.

Fig. 4 shows that pure AP HC bio-oil consists of 50 % furans, 19 % ketones, and 12 % benzenes, 12 % phenols, and no carboxylic acids (CA). Pure DW HC bio-oil contains 66 % CA, 13 % benzenes and 13 % hydrocarbons. BS HC bio-oil comprises 50 % phenols, 17 % ketones, 14 % benzenes and 10 % furan, and CP HC bio-oil consists of 22 % benzenes, 28 % CA, and 40 % phenols. In pathway 2, when CP are pyrolyzed raw, the bio-oil contains 66 % CA and 13 % hydrocarbons. The structure of the biomass feedstocks dictates the reactions that occur during HTC. Of the three building blocks of biomass, cellulose, lignin, and hemicellulose, AP and DW are primarily cellulosic materials (Sebastián-Nicolás et al., 2020; Tulej and Głowacki, 2022), while CP has an equal mixture of lignin, cellulose, and hemicellulose (Duman et al., 2011), and BS is 44 % cellulose, 29 % hemicellulose, and 18 % lignin (Paschos et al., 2022). During HTC, it is likely that decarboxylation reactions produced aromatic groups such as benzenes and phenols, which explains the difference in composition versus CP bio-oils. The bio-oil derived from raw BS has fewer differences from the BS HC bio-oil, with a decrease in alcohols and increase in benzenes and ketones after HTC. The concentration of phenolic compounds in the bio-oil is not altered when BS is carbonized. To determine the synergistic effects that co-pyrolysis may have had on the bio-oil, experimental and predicted concentrations of the various compound types are reported in Fig. 4.

3.3.1. Bio-oil O/C and H/C ratios

An indicator of bio-oil quality is the atomic ratios of oxygen/hydrogen and carbon (O/C and H/C). Pyrolysis bio-oils often require downstream deoxygenation for use in existing energy infrastructure. Additionally, saturated hydrocarbons are the most energetically valuable compound class, so it is therefore of interest to know the relative ratios of O/C and H/C. O/C atomic ratios for bio-oil generally range between 0.1 and 1 while H/C ratios range from 1 to 2 (Negahdar et al., 2016). In this study, O/C values do not exceed 0.3 and H/C values are within 1.3 – 1.8, showing O/C values to be on the low end of the range for chars, and H/C values in the middle of the expected range for chars. AP HC and dry waste mixtures in pathway 1 had lower oxygen and higher hydrogen content than predicted, as seen in the residuals plot in Fig. 2. This shift in ratios indicates the occurrence of deoxygenation and hydrogenation reactions. Notably, the mixtures' atomic ratios are all improved relative to the AP atomic ratios, despite AP being present in 80 or 90 % in the mixtures. The AP/CP mixtures had the most favorable atomic ratios with O/C values < 0.10 and H/C values > 1.6. These particular ratios are similar to previous studies of pyrolyzed hydrochar (Weihrich et al., 2022).

In pathway 2 the experimental and predicted atomic ratios had similar values. While 20/80 AP HC/BS showed positive synergy (Fig. 2), the other experimental values fell just below their predictions. The atomic ratios were also generally lower than the raw CP and BS, which had H/C ratios of nearly 1.8 and O/C ratios of less than 0.1. With the exception of 20/80 AP HC/BS, the atomic ratios of the mixtures shifted towards higher O/C values, indicating an increase in the oxygen content of the bio-oil relative to pure CP and BS feedstock. Coupled with the O/C values of the biochar, it is confirmed that oxygen is devolatilized into the bio-oil and out of the char. The AP HC feedstock has relatively high O/C and low H/C atomic ratios, while the biochar mixtures containing AP HC all showed higher ratios than the pure feedstock. The addition of AP HC to the raw biomass feedstock showed a negative synergistic effect in which the atomic ratios of O/C and H/C increased and decreased, respectively.

A similar pattern to AP HC in the atomic ratios emerges for DW HC in which pathway 1 values are typically higher than predicted, while pathway 2 experimental values are lower than predicted and do not exceed raw CP and BS values. CP-containing mixtures in particular have lower values, which may be due to the presence of fatty acids and ester groups in CP bio-oil which have several oxygen molecules per compound.

3.3.2. AP mixtures

The most notable synergistic effect appears in the pathway 1 90/10 AP/CP bio-oil, where CA are approximately 80 % of the bio-oil, nearly 70 % higher in concentration than predicted. In this bio-oil, furans are not present, despite the additive model (Equation (2) indicating furans to make up nearly half of the bio-oil composition. When the AP/CP ratio is 80/20, the composition shifts towards more phenol groups, and the CA concentration decreases to 30 % of the total composition. During pyrolysis, phenols are formed as lignin begins to decompose at temperatures as low as 190 °C (Yang et al., 2007), while functional groups including alcohols, aldehydes, organic acids, ketones, furans, and esters are formed via cellulose and hemicellulose decomposition. As CP contain more lignin than AP, the addition of 10 % more CP to the mixture may have caused a synergistic decomposition of lignin to produce the relatively high phenol content observed (Kim and Park, 2020). During carbonization, hemicellulose begins to decompose at 180 °C, cellulose degradation begins at 200 °C, while lignin has very little conversion (Funke and Ziegler, 2010). During HTC, lignin decomposition may have been increased by the presence of acidic compounds from the AP.

In Pathway 2, in the AP HC/BS mixtures, both phenol and ketone groups are higher than predicted, while furan and benzene concentrations are lower than predicted. The ketone fraction is largely comprised of cyclopentenone groups, a degradation product of 5-HMF during carbonization (Dutta and Subray Bhat, 2021). During pyrolysis of AP HC/BC, cyclopentenone groups reported to be a significant fraction in the volatile matter on the surface of the hydrochar, are likely volatilized from the surface of the hydrochar and collected in the bio-oil (Becker et al., 2013). The AP HC/CP mixtures in pathway 2 show a change in bio-oil carboxylic acid concentrations. Starting with raw CP (non-carbonized), CA account for 60 % of the bio-oil, while the other functional groups remain in the 5–10 % range each. Hydrocarbons comprise 10 % of the total raw CP bio-oil. For the AP HC/CP mixtures in pathway 2, acid concentrations are higher than predicted, and furan concentrations are lower. Benzene and phenol concentrations are 5–10 % higher than predicted and hydrocarbons are 10 % lower. The ketone concentration is higher than predicted for 80/20 AP/CP but lower for the 50/50 mixture, despite AP contributing most of the ketone concentration, based on the pure feedstock bio-oils. For the 50/50 AP HC/CP bio-oil sample, furan concentration is a bit higher, likely due to the 30 % increase in AP HC and therefore higher carbohydrate content in the mixture, which is known to decompose to furan groups, particularly 5-hydroxymethylfurfural, during pyrolysis (Nomura et al., 2021).

The AP HC/BS has the same pattern with respect to ketone concentrations as the AP HC/CP mixtures; with additional AP HC added, the ketone concentration decreases. In the 20/80 AP HC/BS mixture in pathway 1, alcohol concentrations are nearly 20 % higher than predicted, and benzenes, acids, and furans are lower than predicted. In pathway 2 it appears that synergistic reactions take place that favor the production of compounds from the dry wastes. Phenol in particular is consistently above the predicted concentrations for AP HC/BS mixtures as the hydrochar likely promoted devolatilization of the dry biomass.

3.3.3. DW mixtures

The DW HC bio-oil is concentrated in CA (65 %), largely due to high concentrations of palmitic and oleic acids; the remaining 35 % is primarily benzenes, hydrocarbons, and N-containing compounds. The pathway 1 DW and dry waste mixtures have lower acid concentrations than predicted, with phenols, ketones, and furans higher than predicted.

The selectivity towards phenols may be due to the lignin decomposition during HTC, which forms phenols that likely deposit on the surface of the hydrochar as secondary char and ultimately volatilize during pyrolysis. While DW comprises 80–90 % of the respective mixtures, the combination of DW with CP or BS appears to synergistically increase the production of phenols during HTC and decrease the acid concentration, an important step towards producing more practical biofuels.

Pathway 2 has the opposite effect on acids, particularly for the DW HC/CP mixtures, where acids make up > 70 % of the bio-oil and are 10 % higher in concentration than predicted. Hydrocarbon yields are lower than predicted, showing that a pyrolysis feedstock of DW HC and raw CP has negative synergistic effects on bio-oil composition, in that the experimental value is lower than the predicted additive value. The DW HC/BS mixtures show a different type of synergy as phenol concentrations are increased and acids are decreased relative to predicted values. Furan and benzene groups were produced in higher concentrations than predicted, which points to enhanced cellulosic decomposition of BS producing more furans.

3.4. Discussion of synergistic behavior

Using the additive scheme shown in Eq (1)., experimental results were compared to predicted additive results to study potential synergistic influences that may have occurred throughout the valorization schemes in pathways 1 and 2. First, in Fig. 1 the hydrochar yields are generally higher than predicted, with the exception of AP and CP, which produced 16–18 % HC but was expected to produce ~ 24 % HC. The literature on co-carbonizing biomasses is inconclusive on synergism occurring during co-carbonization to alter yields (C et al., 2019; Zhang et al., 2021). In this work, patterns do emerge: the incorporation of BS increases HC yield above predicted values each time it is used. Unlike HHV and fixed carbon content, HC yield does not appear to be linked to lignin content. This synergy between BS-containing feedstocks and increased hydrochar yield may be due to enhanced Maillard reactions wherein amino acids and saccharides react and the products condense. Sugars from DW/AP and organic acids derived from proteins in BS undergo decarboxylation and dehydration reactions to form the cyclopentanone derivatives, furanone derivatives, and monocyclic aromatics, which then undergo ring condensation and dehydration to form larger aromatic clusters that accumulate to form hydrochar.

Biochars with AP in pathway 1 show lower solid yields than predicted, particularly when increased dry waste was included. This may be due to mass transfer being inhibited during HTC and increased devolatilization when a mixture of AP HC and dry wastes is treated via pyrolysis. DW-based biochars in pathway 1 typically had higher yields than predicted. In pathway 2, biochar yields were higher than predicted as well. Furthermore, fixed carbon was higher than predicted for all pathway 2 mixtures, ranging from 65 to 85 %, as well as for most samples in pathway 1, with the exception of AP/CP mixtures (Fig. 5). Overall, this data shows that pathway 2 synergistically increases not only the biochar yield but the amount of the more stable fixed carbon in said biochar. This is also true for DW-based mixtures in pathway 1, although the volatile matter content was higher than predicted for these mixtures. VM content in pathway 2 was generally within 1 % of the predicted value, except for DW-based mixtures, particularly DW HC/BS mixtures which were lower than predicted.

O/C atomic ratios for both pathways were lower than predicted (Fig. 2), further showing that valorizing mixed feedstocks synergistically improves stability of biochars. However H/C ratios were much lower than predicted for pathway 2 which may indicate that these materials produce a lower value solid fuel than predicted. The observed decrease in O/C but not H/C ratios indicates that decarboxylation reactions occur to decrease oxygenated groups and increase the relative concentration of aromatic groups. This explanation supports the increased hydrochar yield observed. A decrease in both O/C and H/C points to increased dehydration reactions during HTC (Du et al., 2023). As the biochar in pathway 2 shows lower O/C and H/C ratios than pathway 1, pyrolysis is likely the cause of increased dehydration reactions, which is consistent with the varying valorization pathways (Liang et al., 2023). The HHV for pathway 2 values were generally higher than predicted, indicating that the fuel density is perhaps not impacted by the lower H/C. pathway 1 HHV values were mainly higher than predicted as well (Fig. 2).

Synergistic interactions appear in both pathways investigated. In pathway 1 solid yield and fixed carbon were synergistically increased, which may facilitate the biochar's use as an environmental adsorbent or amendment in addition to its solid fuel potential. For pathway 2, fixed carbon and O/C atomic ratio was synergistically improved, but H/C values and biochar yield were less than the additive model predicts, therefore its solid fuel potential may be lower than pathway 1.

4. Conclusions

Two biomass valorization pathways were employed to evaluate the solid and liquid fuel potential of resulting biochar and bio-oil. Pathway 1 hydrothermally carbonized mixed biomasses to produce a hydrochar that was pyrolyzed. Biochar had lower volatile matter and higher HHV values than predicted by an additive model. Bio-oil had lower acids and O/C ratios than predicted. In the second pathway, pyrolyzing a mixture of wet-waste hydrochar with raw dry biomass generated biochar with lower HHV than pathway 1 and a bio-oil with more acids. Pathway 1

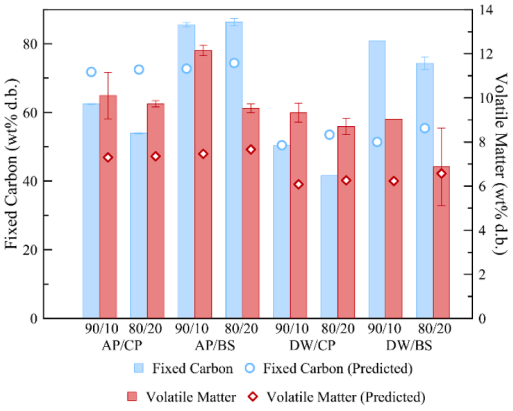

a. Actual and predicted proximate analysis results for pathway 1

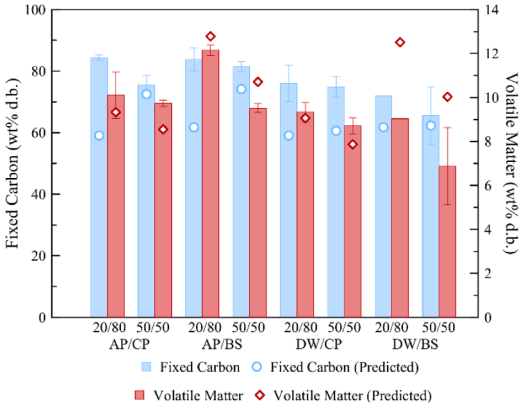

b. Actual and predicted proximate analysis results for pathway 2

Fig. 5. Evidence of synergy between biomasses and pathway 1 and pathway 2 as noted through fixed carbon and volatile matter content.

showed a higher potential for fuel production due to pre-treating with carbonization.

CRediT authorship contribution statement

Madeline Karod: Conceptualization, Data curation, Formal analysis, Investigation, Methodology, Validation, Writing – original draft. **Samantha F. Rubin:** Investigation, Methodology, Writing – original draft. **Jillian L. Goldfarb:** Conceptualization, Resources, Writing – review & editing, Supervision, Funding acquisition.

Declaration of competing interest

The authors declare the following financial interests/personal relationships which may be considered as potential competing interests: Jillian L. Goldfarb reports financial support was provided by USDA National Institute of Food and Agriculture and the US National Science Foundation.

Data availability

Data will be made available on request.

Acknowledgements

This work was supported by a Hatch Grant under accession number 1021398 from the USDA National Institute of Food and Agriculture and from the National Science Foundation (NSF), grant number CBET-2031710, and the Cornell University Engineering Learning Initiatives Program.

Appendix A. Supplementary data

Supplementary data to this article can be found online at https://doi.org/10.1016/j.biortech.2023.130173.

References

Ahmad, M., Rajapaksha, A.U., Lim, J.E., Zhang, M., Bolan, N., Mohan, D., Vithanage, M., Lee, S.S., Ok, Y.S., 2014. Biochar as a sorbent for contaminant management in soil and water: A review. Chemosphere 99, 19–33. https://doi.org/10.1016/J.CHEMOSPHERE.2013.10.071.

Anyaoha, K.E., 2022. Synergistic perspective on biomass co-utilization in thermochemical processes. Bioresource Technology Reports 18, 101043. https://doi.org/10.1016/J.BITEB.2022.101043.

Bardhan, M., Novera, T.M., Tabassum, M., Islam, M.A.A., Islam, M.A.A., Hameed, B.H., 2021. Co-hydrothermal carbonization of different feedstocks to hydrochar as potential energy for the future world: A review. J. Clean. Prod. 298, 126734 https://doi.org/10.1016/j.jclepro.2021.126734.

Becker, R., Dorgerloh, U., Helmis, M., Mumme, J., Diakité, M., Nehls, I., 2013. Hydrothermally carbonized plant materials: Patterns of volatile organic compounds detected by gas chromatography. Bioresour. Technol. 130, 621–628. https://doi.org/10.1016/j.biortech.2012.12.102.

C, H., Z, Z., C, G., W, L., Y, T., X, Z., R, Q., 2019. Synergistic effect of hydrothermal co-carbonization of sewage sludge with fruit and agricultural wastes on hydrochar fuel quality and combustion behavior. Waste management (New York, N.Y.) 100, 171–181. doi: 10.1016/J.WASMAN.2019.09.018.

Cao, Y., He, M., Dutta, S., Luo, G., Zhang, S., Tsang, D.C.W., 2021. Hydrothermal carbonization and liquefaction for sustainable production of hydrochar and aromatics. Renew. Sustain. Energy Rev. 152, 111722 https://doi.org/10.1016/j.rser.2021.111722.

Chen, X., Zhang, Y., Xu, B., Li, Y., 2022. A simple model for estimation of higher heating value of oily sludge. Energy 239, 121921. https://doi.org/10.1016/j.energy.2021.121921.

Cruz-lopes, L., Dulyanska, Y., Domingos, I., Ferreira, J., Fragata, A., Guiné, R., Esteves, B., 2022. Influence of Pre-Hydrolysis on the Chemical Composition of Prunus avium Cherry Seeds. Agronomy 2022, Vol. 12, Page 280 12, 280. doi: 10.3390/AGRONOMY12020280.

Dimitriadis, A., Bergvall, N., Johansson, A.C., Sandström, L., Bezergianni, S., Tourlakidis, N., Meca, L., Kukula, P., Raymakers, L., 2023. Biomass conversion via ablative fast pyrolysis and hydroprocessing towards refinery integration: Industrially relevant scale validation. Fuel 332, 126153. https://doi.org/10.1016/J.FUEL.2022.126153.

Dodds, W.K., Bouska, W.W., Eitzmann, J.L., Pilger, T.J., Pitts, K.L., Riley, A.J., Schloesser, J.T., Thornbrugh, D.J., 2009. Eutrophication of U.S. freshwaters: analysis of potential economic damages. Environ. Sci. Tech. 43, 12–19. https://doi.org/10.1021/ES801217Q.

Du, S., Zhang, Q., Ye, W., Wang, Z., Liu, Z., Huang, J., Xu, X., Wu, Y., Lin, X., He, Q.S., Nanda, S., Changotra, R., Hu, Y., Zhao, Z., Yang, J., 2023. Advancing hydrochar production and application: A critical examination of microwave irradiation and blended feedstocks synergy. J. Clean. Prod. 426, 139049 https://doi.org/10.1016/j.jclepro.2023.139049.

Duman, G., Okutucu, C., Ucar, S., Stahl, R., Yanik, J., 2011. The slow and fast pyrolysis of cherry seed. Bioresour. Technol. 102, 1869–1878. https://doi.org/10.1016/J.BIORTECH.2010.07.051.

Dutta, S., Subray Bhat, N., 2021. Catalytic Transformation of Biomass-Derived Furfurals to Cyclopentanones and Their Derivatives: A Review. doi: 10.1021/acsomega.1c05861.

Farru, G., Cappai, G., Carucci, A., De Gioannis, G., Asunis, F., Milia, S., Muntoni, A., Perra, M., Serpe, A., 2022. A cascade biorefinery for grape marc: recovery of materials and energy through thermochemical and biochemical processes. Sci. Total Environ. 846, 157464 https://doi.org/10.1016/J.SCITOTENV.2022.157464.

Funke, A., Ziegler, F., 2010. Hydrothermal carbonization of biomass: A summary and discussion of chemical mechanisms for process engineering. Biofuels Bioprod. Biorefin. 4, 160–177. https://doi.org/10.1002/BBB.198.

Goldfarb, J.L., Buessing, L., Gunn, E., Lever, M., Billias, A., Casoliba, E., Schievano, A., Adani, F., 2017. Novel Integrated Biorefinery for Olive Mill Waste Management: Utilization of Secondary Waste for Water Treatment. ACS Sustain. Chem. Eng. 5, 876–884. https://doi.org/10.1021/ACSSUSCHEMENG.6B02202.

Jiang, H., Lu, P., Xue, Z., Zhao, D., Bu, C., Ge, H., Song, T., 2022. Prediction and evaluation on fuel properties and pyrolysis characteristics of combustible industrial solid wastes. J. Energy Inst. 105, 232–241. https://doi.org/10.1016/j.joei.2022.09.010.

Kambo, H.S., Dutta, A., 2015. A comparative review of biochar and hydrochar in terms of production, physico-chemical properties and applications. Renew. Sustain. Energy Rev. 45, 359–378. https://doi.org/10.1016/J.RSER.2015.01.050.

Kassem, N., Pecchi, M., Maag, A.R., Baratieri, M., Tester, J.W., Goldfarb, J.L., 2022. Developing Decision-Making Tools for Food Waste Management via Spatially Explicit Integration of Experimental Hydrothermal Carbonization Data and Computational Models Using New York as a Case Study. ACS Sustain. Chem. Eng. 10, 16578–16587. https://doi.org/10.1021/ACSSUSCHEMENG.2C04188/ASSET/IMAGES/LARGE/SC2C04188_0006.JPEG.

Kim, J.-S., Park, K.-B., 2020. Production of Phenols by Lignocellulosic Biomass Pyrolysis 289–319. doi: 10.1007/978-981-15-2732-6_11.

Klemm, M., Kröger, M., Görsch, K., Müller-Langer, F., Majer, S., 2020. Fuel-Driven Biorefineries Using Hydrothermal Processes. Chem.-Ing.-Tech. https://doi.org/10.1002/cite.202000093.

Liang, J., Lin, H., Li, C., Zhang, L., Zhang, S., Wang, S., Xiang, J., Hu, S., Wang, Y., Hu, X., 2023. Interaction of derivatives of cellulose and lignin in co-HTC, co-pyrolysis and co-activation. Fuel 351, 129033. https://doi.org/10.1016/j.fuel.2023.129033.

Lin, J.C., Mariuzza, D., Volpe, M., Fiori, L., Ceylan, S., Goldfarb, J.L., 2021. Integrated thermochemical conversion process for valorizing mixed agricultural and dairy waste to nutrient-enriched biochars and biofuels. Bioresour. Technol. 328, 124765 https://doi.org/10.1016/J.BIORTECH.2021.124765.

Liu, Z., Quek, A., Kent Hoekman, S., Balasubramanian, R., 2013a. Production of solid biochar fuel from waste biomass by hydrothermal carbonization. Fuel 103, 943–949. https://doi.org/10.1016/j.fuel.2012.07.069.

Liu, Z., Quek, A., Parshetti, G., Jain, A., Srinivasan, M.P., Hoekman, S.K., Balasubramanian, R., 2013b. A study of nitrogen conversion and polycyclic aromatic hydrocarbon (PAH) emissions during hydrochar–lignite co-pyrolysis. Appl. Energy 108, 74–81. https://doi.org/10.1016/J.APENERGY.2013.03.012.

Mondal, C., Pal, S.K., Samanta, B., Dutta, D., Raj, S., 2023. Analysis and significance of prediction models for higher heating value of coal: an updated review. J. Therm. Anal. Calorim. 148, 7521–7538. https://doi.org/10.1007/s10973-023-12272-4.

Negahdar, L., Gonzalez-Quiroga, A., Otyuskaya, D., Toraman, H.E., Liu, L., Jastrzebski, J. T.B.H., Van Geem, K.M., Marin, G.B., Thybaut, J.W., Weckhuysen, B.M., 2016. Characterization and Comparison of Fast Pyrolysis Bio-oils from Pinewood, Rapeseed Cake, and Wheat Straw Using 13C NMR and Comprehensive GC × GC. ACS Sustain. Chem. Eng. 4, 4974–4985. https://doi.org/10.1021/ACSSUSCHEMENG.6B01329/SUPPL_FILE/SC6B01329_SI_001.PDF.

Nomura, T., Minami, E., Kawamoto, H., 2021. Hydroxymethylfurfural as an Intermediate of Cellulose Carbonization. ChemistryOpen 10, 610–617. https://doi.org/10.1002/OPEN.202000314.

Paschos, T., Louloudi, A., Papayannakos, N., Kekos, D., Mamma, D., 2022. Potential of barley straw for high titer bioethanol production applying pre-hydrolysis and simultaneous saccharification and fermentation at high solid loading. Biofuels 13, 467–473. https://doi.org/10.1080/17597269.2020.1760688.

Pecchi, M., Baratieri, M., Goldfarb, J.L., Maag, A.R., 2022. Effect of solvent and feedstock selection on primary and secondary chars produced via hydrothermal carbonization of food wastes. Bioresour. Technol. 348, 126799 https://doi.org/10.1016/J.BIORTECH.2022.126799.

Polin, J.P., Carr, H.D., Whitmer, L.E., Smith, R.G., Brown, R.C., 2019. Conventional and autothermal pyrolysis of corn stover: Overcoming the processing challenges of high-ash agricultural residues. J. Anal. Appl. Pyrol. 143, 104679 https://doi.org/10.1016/J.JAAP.2019.104679.

Pollard, Z.A., Goldfarb, J.L., 2021. Valorization of cherry pits: Great Lakes agro-industrial waste to mediate Great Lakes water quality. Environ. Pollut. 270, 116073 https://doi.org/10.1016/J.ENVPOL.2020.116073.

Proximate Analysis, 2015. . Handbook of Coal Analysis 116–143. doi: 10.1002/9781119037699.CH5.

Renhe, I.R.T., Perrone, Í.T., Tavares, G.M., Schuck, P., De Carvalho, A.F., 2019. Physicochemical Characteristics of Raw Milk. Raw Milk: Balance Between Hazards and Benefits 29–43. doi: 10.1016/B978-0-12-810530-6.00002-X.

Reza, M.T., Lynam, J.G., Uddin, M.H., Coronella, C.J., 2013. Hydrothermal carbonization: Fate of inorganics. Biomass Bioenergy 49, 86–94. https://doi.org/10.1016/J.BIOMBIOE.2012.12.004.

Sebastián-Nicolás, J.L., González-Olivares, L.G., Vázquez-Rodríguez, G.A., Lucho-Constatino, C.A., Castañeda-Ovando, A., Cruz-Guerrero, A.E., 2020. Valorization of whey using a biorefinery. Biofuels Bioprod. Biorefin. 14, 1010–1027. https://doi.org/10.1002/BBB.2100.

Shi, H., Mahinpey, N., Aqsha, A., Silbermann, R., 2016. Characterization, thermochemical conversion studies, and heating value modeling of municipal solid waste. Waste Manag. 48, 34–47. https://doi.org/10.1016/J.WASMAN.2015.09.036.

Silva, R.D.V.K., Lei, Z., Shimizu, K., Zhang, Z., 2020. Hydrothermal treatment of sewage sludge to produce solid biofuel: Focus on fuel characteristics. Bioresource Technology Reports 11, 100453. https://doi.org/10.1016/J.BITEB.2020.100453.

Sun, X.F., Jing, Z., Fowler, P., Wu, Y., Rajaratnam, M., 2011. Structural characterization and isolation of lignin and hemicelluloses from barley straw. Ind. Crop. Prod. 33, 588–598. https://doi.org/10.1016/J.INDCROP.2010.12.005.

Tulej, W., Głowacki, S., 2022. Analysis of Material-Characterization Properties of Post-Production Waste—The Case of Apple Pomace. Materials 2022, Vol. 15, Page 3532 15, 3532. doi: 10.3390/MA15103532.

Ul Saqib, N., Sarmah, A.K., Baroutian, S., 2019. Effect of temperature on the fuel properties of food waste and coal blend treated under co-hydrothermal carbonization. Waste Manag. 89, 236–246. https://doi.org/10.1016/J.WASMAN.2019.04.005.

Weihrich, S., Xing, X., Zhang, X., 2022. Co-pyrolysis and HTC refined biomass-biosolid-mixes: combustion performance and residues. Int. J. Energy Environ. Eng. https://doi.org/10.1007/s40095-021-00453-6.

Xiu, S., Shahbazi, A., 2012. Bio-oil production and upgrading research: A review. Renew. Sustain. Energy Rev. 16, 4406–4414. https://doi.org/10.1016/J.RSER.2012.04.028.

Yang, H., Yan, R., Chen, H., Lee, D.H., Zheng, C., 2007. Characteristics of hemicellulose, cellulose and lignin pyrolysis. Fuel 86, 1781–1788. https://doi.org/10.1016/J.FUEL.2006.12.013.

Yao, Z., Ma, X., Wu, Z., Yao, T., 2017. TGA–FTIR analysis of co-pyrolysis characteristics of hydrochar and paper sludge. J. Anal. Appl. Pyrol. 123, 40–48. https://doi.org/10.1016/J.JAAP.2016.12.031.

Zhang, B., Heidari, M., Regmi, B., Salaudeen, S., Arku, P., Thimmannagari, M., Dutta, A., 2018. Hydrothermal Carbonization of Fruit Wastes: A Promising Technique for Generating Hydrochar. Energies 2018, Vol. 11, Page 2022 11, 2022. doi: 10.3390/EN11082022.

Zhang, C., Zheng, C., Ma, X., Zhou, Y., Wu, J., 2021. Co-hydrothermal carbonization of sewage sludge and banana stalk: Fuel properties of hydrochar and environmental risks of heavy metals. J. Environ. Chem. Eng. 9, 106051 https://doi.org/10.1016/J.JECE.2021.106051.

Zhou, Z., Bu, Y., Long, X., Cai, J., 2023. N-containing biochar from oatmeal: hydrothermal synthesis and used as highly efficient adsorbent for Cr(VI) adsorptive-reduction removal. Biomass Convers. Biorefin. 1–10 https://doi.org/10.1007/S13399-023-03955-X/METRICS.